Inorg. Chem. **2004**, *43*, 1250−1256

Syntheses and Solid-State and Solution Structures of $[Ba\{(C_5Me_5)_2Ti_2F_7\}_2(hmpa)]$ and $[Ba_8Ti_6F_{30}I_2(C_5Me_5)_6(hmpa)_6][I_3]_2$

Andrej Pevec*

Faculty of Chemistry and Chemical Technology, University of Ljubljana, Aškerčeva 5, Ljubljana, Slovenia

Received October 30, 2003

The complexes $[Ba\{(C_5Me_5)_2Ti_2F_7\}_2(hmpa)]\cdot(THF)$, **1**·hmpa·(THF), and $[Ba_8Ti_6F_{30}I_2(C_5Me_5)_6(hmpa)_6][I_3]_2\cdot 10(THF)$, **2**$[I_3]_2\cdot 10(THF)$, were prepared from $[Hdmpy]^+[(C_5Me_5)_2Ti_2F_7]^-$ (dmpy = 2,6-dimethylpyridine), BaI_2, and hmpa (hmpa = hexamethylphosphoramide). They were characterized by ^1H and ^{19}F NMR and IR spectroscopy and examined by single-crystal X-ray crystallography. The complexation equilibrium of the barium ion in **1** with hmpa and the dynamics of the barium ion moving on the fluorine surfaces of $[(C_5Me_5)_2Ti_2F_7]^-$ in **1**·hmpa have been studied by variable-temperature ^{19}F NMR spectroscopy. The core of the complex **2**$[I_3]_2\cdot 10(THF)$ resembles the basic structural unit of the cubic perovskite.

Introduction

Perovskite structures of the ABX_3 compounds (A, B = metal cations; X = anion) with corner-shared octahedra BX_6 and larger A cations filling the 12-fold coordination holes among the octahedra are known for about 90% of the metals.[1] Metal oxides with perovskite structure are intensively studied because of their electrical, magnetic, and optical properties.[2] The thin layers and nanocrystals of perovskite oxides revealed particle-size dependency of their properties.[3] The molecular clusters with metal−oxo cores of small +3- and +4-charged metal (B type) have been intensively studied.[4,5] The core of these clusters approaches the lower limit of the dimensions of nanoclusters and could be seen as well-defined intermediates in the "bottom-up" preparation of nanosized metal oxides.[6] In contrast, the clusters with the core built from both A- and B-type perovskite cations incorporate only a few (up to four) oxo ligands.[7] Apparently, the partial substitution of highly charged cations in the cluster core with large A-type cations increases the number of coordination sites on metals, decreases the positive charge, and therefore favors −1 and neutral ligands instead of O^{2-} ligands. Therefore, F^- ligand, with a similar ionic radius and also isoelectronic to O^{2-}, could be a suitable substitute for oxo ligands in the preparation of clusters with the core, incorporating large cations and possibly structurally resembling the perovskite oxides. Recently, organometallic complexes with the core built from Na, Ti, and F atoms have been reported.[8]

Herein, the preparation and structural properties of the two novel organometallic clusters are reported as $[Ba\{(C_5Me_5)_2Ti_2F_7\}_2(hmpa)]\cdot(THF)$, **1**·hmpa·(THF), and $[Ba_8Ti_6F_{30}I_2$-

* E-mail: andrej.pevec@uni-lj.si.

(1) Tejuca, L. G.; Fierro, J. L. G. *Perovskites and Applications of Perovskite-type Oxides*; Marcel Dekker: New York, 1992. (b) Peña, M. A.; Fierro, J. L. G. *Chem. Rev.* **2001**, *101*, 1981−2017.
(2) McCarroll, W. H. In *Encyclopedia of Inorganic Chemistry*; King, R. B., Ed.; Wiley: Chichester, U.K., 1994; Vol. 6, pp 2903−2946.
(3) Wang, R. H.; Zhu, Y. M.; Shapiro, S. M. *Phys. Rev. Lett.* **1998**, *80*, 2370−2373. (b) Tsunekawa, S.; Ito, S.; Mori, T.; Ishikawa, K.; Li, Z.-Q.; Kawazoe, Y. *Phys. Rev. B: Condens. Matter* **2000**, *62*, 3065−3070. (c) Zhang, J.; Yin, Z.; Zhang, M.-S.; Scott, J. F. *Solid State Commun.* **2001**, *118*, 241−246. (d) Urban, J. J.; Yun, W. S.; Gu, Q.; Park, H. *J. Am. Chem. Soc.* **2002**, *124*, 1186 and 1187.
(4) Winpenny, R. E. P. *Adv. Inorg. Chem.* **2001**, *52*, 1−111. (b) Benelli, C.; Parsons, S.; Solan, G. A.; Winpenny, R. E. P. *Angew. Chem., Int. Ed. Engl.* **1996**, *35*, 1825−1828. (c) Parsons, S.; Smith, A. A.; Winpenny, R. E. P. *Chem. Commun.* **2000**, 579 and 580.
(5) Nair, V. S.; Hagen, K. S. *Inorg. Chem.* **1994**, *33*, 185 and 186 and references therein. (b) Caneschi, A.; Cornia, A.; Fabretti, A. C.; Gatteschi, D. *Angew. Chem., Int. Ed. Engl.* **1996**, *34*, 2716−2718. (c) Aromí, G.; Aubin, S. M. J.; Bolcar, M. A.; Christou, G.; Eppley, H. J.; Folting, K.; Hendrickson, D. N.; Huffman, J. C.; Squire, R. C.; Tsai, H.-L.; Wang, S.; Wemple, M. W. *Polyhedron* **1998**, *17*, 3005−3020.
(6) Schubert, U. *Chem. Mater.* **2001**, *13*, 3487−3494. (b) Kickelbick, G.; Feth, M. P.; Bertagnolli, H.; Puchberger, M.; Holzinger, D.; Gross, S. *J. Chem. Soc., Dalton Trans.* **2002**, 3892−3898.
(7) Yanovsky, A. I.; Yanovskaya, M. I.; Limar, V. K.; Kessler, V. G.; Turova, N. Ya.; Struchkov, Y. T. *J. Chem. Soc., Chem. Commun.* **1991**, 1605 and 1606. (b) Gaskins, B.; Lannutti, J. J. *Acta Crystallogr., Sect. C* **1994**, *50*, 1387−1390. (c) Starikova, Z. A.; Yanovsky, A. I.; Kotova, N. M.; Yanovskaya, M. I.; Turova, N. Ya.; Benlian, D. *Polyhedron* **1997**, *16*, 4347−4351. (d) Veith, M. *J. Chem. Soc., Dalton Trans.* **2002**, 2405−2412.
(8) Liu, F.-Q.; Kuhn, A.; Herbst-Irmer, R.; Stalke, D.; Roesky, H. W. *Angew. Chem., Int. Ed. Engl.* **1994**, *33*, 555 and 556. (b) Liu, F.-Q.; Stalke, D.; Roesky, H. W. *Angew. Chem., Int. Ed. Engl.* **1995**, *34*, 1872−1874.

10.1021/ic035256v CCC: $27.50
Published on Web 01/22/2004

$(C_5Me_5)_6(hmpa)_6][I_3]_2$·10(THF), **2**$[I_3]_2$·10(THF) (hmpa = hexamethylphosphoramide), where the barium−titanium−fluorine core of **2** reveals a similarity to the perovskite structure. The variable-temperature (VT) ^{19}F NMR spectra of the **1**·hmpa·(THF) solution show the equilibrium of coordination of the barium ion in **1** by hmpa and the dynamics of the barium ion on the fluorine surface of $[(C_5Me_5)_2Ti_2F_7]^-$ in **1**·hmpa.

Experimental Section

General Procedures. All of the experimental manipulations were carried out under a nitrogen or argon atmosphere using standard Schlenk techniques or a drybox. Solvents were dried over a Na/K alloy and distilled prior to use. Deuterated NMR solvents were treated with CaH_2, distilled, and stored under argon. NMR spectra were recorded on a Bruker DPX 300 spectrometer operating at 300 MHz (^1H) and 282 MHz (^{19}F). Infrared spectra (Nujol) were recorded on a Perkin-Elmer FT-1720X spectrometer. Melting points were measured using a Büchi 535 apparatus and are reported uncorrected. Mass spectrometric analysis was performed on a Micromass Autospec-Q (Manchester, U.K.) double focusing sector mass spectrometer equipped with an electrospray interface, controlled by a Digital Alpha Station 150, using OPUS software. $[Hdmpy]^+[(C_5Me_5)_2Ti_2F_7]^-$ was prepared according to ref 9 (dmpy = 2,6-dimethylpyridine). BaI_2 and hmpa were purchased from Aldrich.

Synthesis. $[Hdmpy]^+[(C_5Me_5)_2Ti_2F_7]^-$ (2 mmol), BaI_2 (1 mmol), and hmpa (1 mmol) were dissolved in THF (50 mL). The resulting orange solution was stirred overnight and then filtered. The composition of the product depends on the crystallization as follows: (a) The orange crystals of **1**·hmpa·(THF) appeared in the solution after slow evaporation of the solvent at reduced pressure (50% yield). (b) The solution was concentrated to 10 mL and stored at 4 °C. The mixture of **1**·hmpa·(THF) and red crystals of **2**$[I_3]_2$·10(THF) were obtained in 10 weeks; **1**·hmpa·(THF) was removed from the mixture by dissolving it in THF [10% yield of **2**$[I_3]_2$·10(THF)]. *Data for **1**·hmpa·(THF).* Decomposition: 190−220 °C. ^1H NMR ($CDCl_3$, 302 K) δ: 3.74 (m, 4H, THF), 2.64 (d, 18H, J_{PH} = 9 Hz, hmpa), 2.10 (s, 60H, C_5Me_5), 1.85 (m, 4H, THF). ^{19}F NMR (toluene-d_8, 302 K) δ: 180.0, 178.6, 75.5, 65.2, 59.5, −35.7, −45.8, −48.0. IR (CsI, Nujol) ν (cm^{-1}): 1296s, 1170b, 1069w, 989b, 752s, 632m, 610vs, 542m, 476s. *Data for **2**$[I_3]_2$·10(THF).* Decomposition: 245−250 °C. ^{19}F NMR (hmpa, 302 K) δ: 27.72 (s, 12F), 12.67 (s, 12F), −52.65 (s, 6F). IR (CsI, Nujol) ν (cm^{-1}): 1292m, 1161m, 989s, 748m, 497vs.

X-ray Crystallography. Crystal data and refinement parameters for **1**·hmpa·(THF) and **2**$[I_3]_2$·10(THF) are listed in Table 1. Selected crystals of **1**·hmpa·(THF) and **2**$[I_3]_2$·10(THF) were quickly mounted on glass fibers and placed in a stream of cold nitrogen. Data were collected on a Nonius Kappa CCD diffractometer equipped with a Mo anode (Kα radiation, λ = 0.710 73 Å) and a graphite monochromator, and the multiscan adsorption correction[10] was performed. The structures were solved by direct methods (SHELX-97) and refined by a full-matrix least-squares procedure based on F^2 (SHELXL-97).[11] All of the non-hydrogen atoms were refined anisotropically, while the hydrogen atoms were included in the model at geometrically calculated positions and refined using a riding model. The hmpa and solvent THF in **1**·hmpa·(THF) are disordered about a 2-fold rotation axis in the structure and were refined with occupancies of 0.5 for all of those atoms. The structure solution and refinement in space group *Cc* (which would not impose any disorder) instead of *C*2/*c* have been considered and have not given successful results. Terminal iodine atoms in the I_3^- anion in **2**$[I_3]_2$·10(THF) were found to be disordered over three positions and were refined with occupancies of 0.33 for all of those atoms. The THF molecules in **2**$[I_3]_2$·10(THF) were refined isotropically with the use of geometric restraints. The residual density peaks (in the vicinity of THF molecules and I_3^- anion) were unrefineable and therefore were not included in the model.

Table 1. Summary of the X-ray Crystallographic Information

	1·hmpa·(THF)	**2**$[I_3]_2$·10(THF)
formula	$C_{50}H_{86}BaF_{14}N_3O_2PTi_4$	$C_{136}H_{278}Ba_8F_{30}I_8N_{18}O_{16}P_6Ti_6$
fw	1387.13	5578.90
crystal system	monoclinic	monoclinic
space group	*C*2/*c* (No. 15)	*C*2/*c* (No. 15)
a (Å)	25.4497(3)	41.1535(5)
b (Å)	11.1503(2)	16.7918(2)
c (Å)	22.6957(3)	33.7062(4)
β (deg)	110.962(1)	109.723(1)
V (Å^3)	6014.16(15)	21 925.9(5)
T (K)	190(2)	150(2)
Z	4	4
D_{calcd} (g cm^{-3})	1.452	1.690
μ(Mo Kα) (mm^{-1})	1.256	2.861
crystal size (mm)	0.10 × 0.10 × 0.10	0.23 × 0.15 × 0.10
θ range (deg)	2.02−27.57	1.57−27.47
data measured, unique (R_{int})	12 891, 6853 (0.0312)	29 651, 20 244 (0.0365)
observed data [$I > 2\sigma(I)$]	5268	14 247
no. of parameters	386	971
R,[a] wR_2[b] [$I > 2\sigma(I)$]	0.0420, 0.1153	0.0761, 0.2037
R, wR_2 (all data)	0.0729, 0.1583	0.1178, 0.2470
S[c]	1.168	1.074
max, min peaks (e Å^{-3})	0.998, −1.560	3.715, −3.876

[a] $R = \sum||F_o| - |F_c||/\sum|F_o|$. [b] $wR_2 = \{\sum[w(F_o^2 - F_c^2)^2]/\sum[w(F_o^2)^2]\}^{1/2}$. [c] $S = \{\sum[(F_o^2 - F_c^2)^2]/(n/p)\}^{1/2}$, where n is the number of reflections and p is the total number of parameters refined.

Results and Discussion

Syntheses and Crystal Structures. The orange crystals of **1**·hmpa·(THF) were obtained in 48 h by slow evaporation of the THF solution containing $[Hdmpy]^+[(C_5Me_5)_2Ti_2F_7]^-$,[9] BaI_2, and hmpa. The red crystals of **2**$[I_3]_2$·10(THF) were obtained in 10 weeks from the solution of the same composition stored at 4 °C. The crystals of **2**$[I_3]_2$·10(THF) are insoluble in THF and chloroform but soluble in hmpa. The structures of **1**·hmpa·(THF) and **2**$[I_3]_2$·10(THF) have been determined by a single-crystal X-ray analysis at low temperature. In the structure of **1**·hmpa·(THF) (Figure 1), two ligands, $[(C_5Me_5)_2Ti_2F_7]^-$ and hmpa, are coordinated to the Ba^{2+} ion with Ba−F and Ba−O distances of 2.664(2)−2.878(2) and 2.653(6) Å, respectively (Table 2). A similar complexation was found in an analogous calcium compound.[12] The structure of **2**$[I_3]_2$·10(THF) is built from heteronuclear centrosymmetric cation **2** (Figure 2) and two triiodide anions. The inorganic core of **2** is covered by the

(9) Perdih, F.; Demšar, A.; Pevec, A.; Petriček, S.; Leban, I.; Giester, G.; Sieler, J.; Roesky, H. W. *Polyhedron* **2001**, *20*, 1967−1971.
(10) Otwinowski, Z.; Minor, W. *Methods Enzymol.* **1997**, *276*, 307−326.
(11) Sheldrick, G. M. *SHELXL-97: Program for Automatic Solution of Crystal Structures*; University of Göttingen: Göttingen, Germany, 1997. (b) Sheldrick, G. M. *SHELXL-97: Program for Crystal Structure Refinement*; University of Göttingen: Göttingen, Germany, 1997.
(12) Demsar, A.; Pevec, A.; Petriček, S.; Golič, L.; Petrič, A.; Björgvinsson, M.; Roesky, H. W. *J. Chem. Soc., Dalton Trans.* **1998**, 4043−4047.

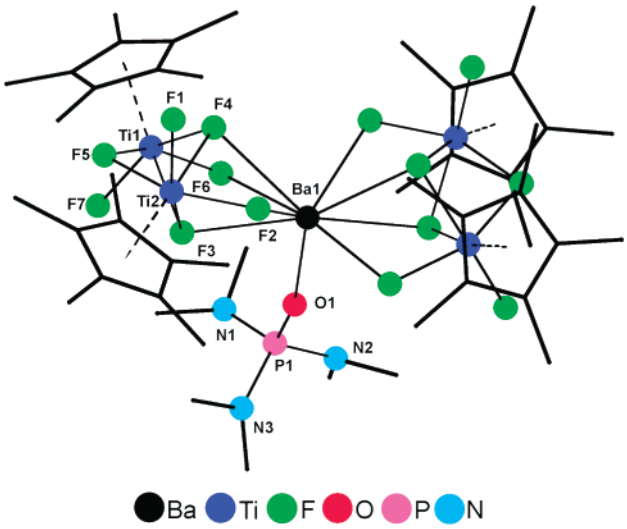

Figure 1. DIAMOND view of **1**·hmpa. The hydrogen atoms of C_5Me_5 and hmpa ligands are not shown. The hmpa molecule is disordered over two positions; only one is shown.

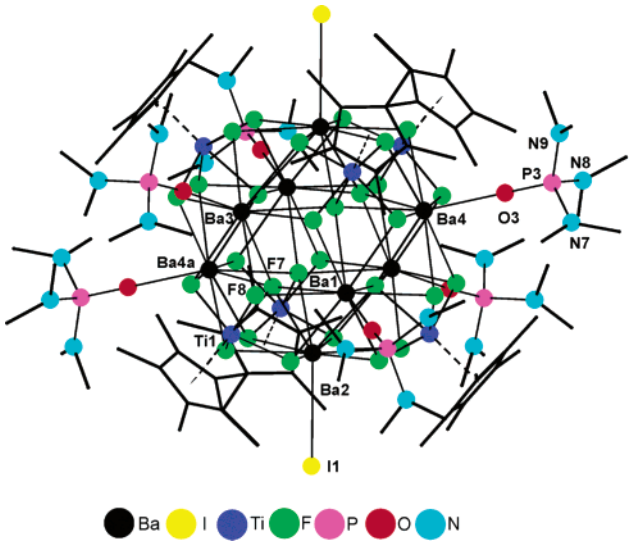

Figure 2. DIAMOND view of **2**. The hydrogen atoms of C_5Me_5 and hmpa ligands are not shown.

Table 2. Selected Bond Distances (Å) and Angles (deg) for **1**·hmpa·(THF)

Ba1−F2	2.664(2)	Ti1−F7	1.834(2)
Ba1−F3	2.734(2)	Ba1−O1	2.653(6)
Ba1−F4	2.878(2)	P1−O1	1.493(6)
Ba1−F6	2.669(2)	P1−N1	1.697(13)
Ti1−F4	2.000(2)	P1−N2	1.645(9)
Ti1−F5	2.021(2)	P1−N3	1.653(9)
Ba1−F4−Ti1	97.73(8)	F3−Ba1−F4	142.11(6)
Ba1−F6−Ti1	108.39(10)	F3−Ba1−O1	80.74(16)
Ti1−F5−Ti2	100.41(10)	Ba1−O1−P1	165.2(4)
F7−Ti1−F4	146.88(10)	O1−P1−N1	116.3(4)

hydrophobic layer of six Ti-bonded C_5Me_5 ligands, six Ba-bonded hmpa ligands, and two Ba-bonded iodide ligands. Cation **2** exhibits approximate D_{3d} symmetry with a 3-fold axis connecting the two iodine-bonded Ba atoms. All of the 30 F atoms in this complex are in bridging positions. The 24 F atoms on the surface of the central bulk bridge two Ba and one Ti atoms [Ba−F distances are in the range of 2.724(6)−2.811(7) Å; Ti−F distances are in the range of

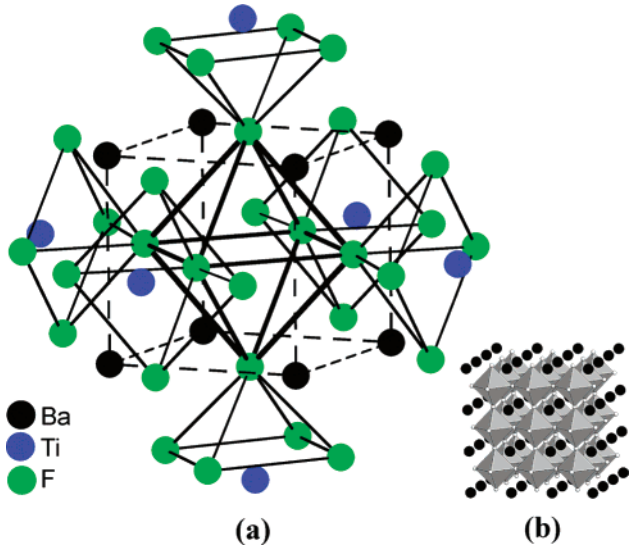

Figure 3. (a) Structure of the $Ba_8Ti_6F_{30}$ core of **2** in the crystal and (b) polyhedral representation of the cubic perovskite structure.

Table 3. Selected Bond Distances (Å) and Angles (deg) for **2**$[I_3]_2$·10(THF)

F7−Ba1	2.849(6)	F8−Ti1	1.955(7)
F7−Ba2	2.835(6)	Ba4−O3	2.588(9)
F7−Ba3	2.811(6)	P3−O3	1.482(9)
F7−Ba4a	2.845(6)	P3−N7	1.669(14)
F7−Ti1	2.165(6)	P3−N8	1.619(14)
F8−Ba1	2.805(7)	P3−N9	1.627(14)
F8−Ba3	2.764(6)	Ba2−I1	3.3946(10)
Ba1−F7−Ba3	89.59(17)	Ba1−F8−Ti1	101.9(3)
Ba1−F7−Ti1	95.4(2)	Ba3−F8−Ti1	102.4(3)
Ba1−F7−Ba4a	169.4(2)	Ba4−O3−P3	175.4(6)
Ba1−F8−Ba3	91.44(19)	O3−P3−N9	110.8(7)

1.924(7)−1.966(7) Å] (Table 3). Each of the six inner F atoms is coordinated to four Ba atoms and one Ti atom [distances of Ba−F are in the range of 2.760(6)−2.870(6) Å; Ti−F distances are in the range 2.165(6)−2.182(6) Å]. The distances Ba−F are in accordance with those in BaF_2 [d(Ba−F) = 2.685 Å, CN(Ba) = 8][13] and in $BaTiF_6$ (2.78−2.94 Å).[14] The molecular compounds with Ba^{2+} ion coordinated by trifluoromethyl and fluorophenyl fluorine-donating atoms were also reported.[15]

The core $Ba_8Ti_6F_{30}$ of **2** is an approximate cube of eight Ba atoms at the corners and six F atoms on its faces. The faces of the cube are capped with TiF_4 moieties (Figure 3a). The cube of eight Ba atoms is nearly regular; the Ba···Ba distances are from 3.9583(9) to 4.0270(9) Å, and angles are from 88.46(2) to 91.63(2)°. The Ba···Ba interatomic distances and the positions of the Ba and F atoms in the Ba_8F_{30} core resemble the packing of Ba and oxygen atoms in the perovskite structure of $BaTiO_3$ (Figure 3b). The arrangement of 38 atoms in the Ba_8F_{30} core also represents a cutoff of the face-centered-cubic packing. The analogous face-centered-cubic structure was calculated to be the most stable arrange-

(13) West, A. R. *Basic Solid State Chemistry*, 2nd ed.; Wiley: Chichester, U.K., 1999.
(14) Becker, S.; Benner, G.; Hoppe, R. *Z. Anorg. Allg. Chem.* **1990**, *591*, 7−16.
(15) Plenio, H. *Chem. Rev.* **1997**, *97*, 3363−3384. (b) Buschmann, H. J.; Hermann, J.; Kaupp, M.; Plenio, H. *Chem.—Eur. J.* **1999**, *5*, 2566−2572.

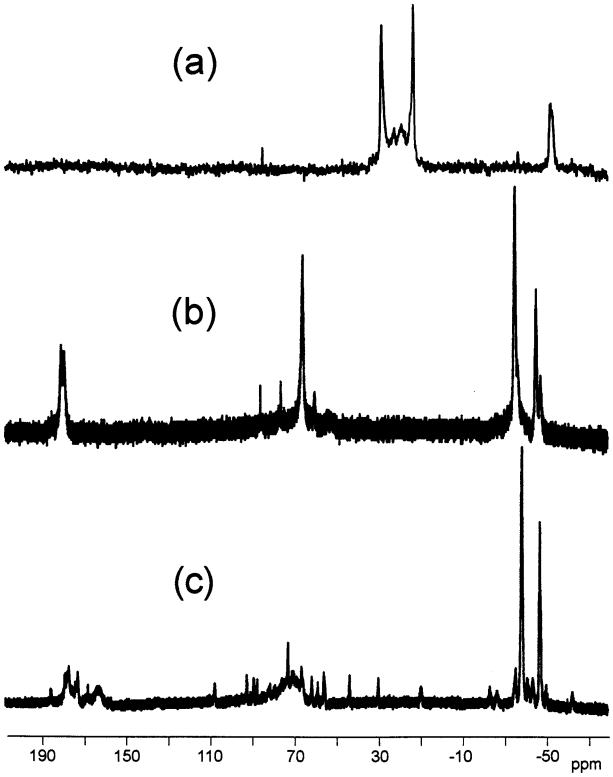

Figure 4. ^{19}F NMR spectra of (a) **2**$[I_3]_2$·10(THF) in the hmpa solution at 302 K, (b) **1**·hmpa·(THF) at 302 K, and (c) **1**·hmpa·(THF) at 222 K (both in the toluene-d_8 solution).

ment of a cluster of 38 atoms.[16] From seven sites in **2**, corresponding to the titanium positions in $BaTiO_3$, six sites are occupied by Ti atoms, while the site in the center of **2** is empty. The atoms in the core of **2** show the following displacements from their positions in an idealized perovskite core structure (using the Ba_8 cube of **2** as a reference): The six inner F atoms surrounding the empty site are shifted for 0.24(1) Å from the faces of the Ba_8 cube toward the Ti atom. The outer F atoms are shifted for 0.14(1) Å toward the inner F ones. The Ti atoms are shifted for 0.42(1) Å away from the center of **2**.

NMR, Mass, and IR Spectra of 2[I$_3$]$_2$·10(THF). The ^{19}F NMR spectrum of **2**$[I_3]_2$·10(THF) in hmpa shows three singlets in the intensity ratio of 2:2:1, which is in accordance with the D_{3d} symmetry of **2** (two sets of 12 equivalent surfaces and six inner fluorine atoms) in solution (Figure 4a). Two broad resonances between two resonances of the surface fluorine atoms likely show the presence of $[Ba_8Ti_6F_{30}I(C_5Me_5)_6(hmpa)_7]^{3+}$, resulting from the exchange of one iodide ligand in **2** by a molecule of the hmpa solvent. The signals of m/z = 1779, 1689, 1600, and 1510 were observed in the electrospray ionization mass spectrum of **2**$[I_3]_2$·10(THF) and correspond to the $[Ba_8Ti_6F_{30}I_2(C_5Me_5)_6(hmpa)_n]^{2+}$ (n = 0−3) fragments. These signals are accompanied by intermediate signals with m/z = 1734, 1645, and 1555 that can be assigned to the splitting of two $[(CH_3)_2NH]$ from $[Ba_8Ti_6F_{30}I_2(C_5Me_5)_6(hmpa)_n]^{2+}$. In addition, the signals of m/z = 3864, 3685, 3506, 3327, and 3147 are assigned to $[Ba_8Ti_6F_{30}I_3(C_5Me_5)_6(hmpa)_n]^+$ (n = 0−4). The formation of this ion can be explained by the binding of I^- (from $[I_3]^-$) to **2**. The intermediate signals m/z = 3775, 3596, 3417, and 3237 can also be recognized as the products of splitting of two $[(CH_3)_2NH]$ from $[Ba_8Ti_6F_{30}I_3(C_5Me_5)_6(hmpa)_n]^+$. The mass spectrum shows that the $[Ba_8Ti_6F_{30}(C_5Me_5)_6]$ core remains intact. Changes occur only in ligands coordinated to barium. Only one IR absorption band at 497 cm^{-1} (overlapped with the hmpa band) in the Ti−F stretching range reflects the high symmetry of the core of **2**.

VT ^{19}F NMR Spectra of the hmpa/1·hmpa Solution. The ^{19}F NMR spectra of **1**·hmpa·(THF) at 302 and 222 K in the 0.02 M toluene-d_8 solution are shown in Figure 4b,c. The spectrum at 302 K shows four major resonances. After the solution was cooled to 222 K, additional resonances appear, suggesting equilibria of a few species in solution. The addition of hmpa to the 0.02 M toluene-d_8 solution of **1**·hmpa·(THF) simplifies the ^{19}F NMR spectra. The VT ^{19}F NMR spectra of hmpa/**1**·hmpa (6:1 molar ratio)[17] in the toluene-d_8 solution are shown in Figures 5a and 6. The ^{19}F NMR spectrum taken at 302 K exhibits four major resonances (intensity ratio 2:2:2:1) and two minor resonances of similar intensities (Figure 5a). The ratio of the intensities of major to minor resonances increases by a temperature decrease or (not shown) by increasing the hmpa/**1**·hmpa ratio. Additionally, after the solution was cooled below 282 K, two major singlet resonances decoalesce to two pairs of singlets (Figure 5a). The shape of the multiplet (δ = −36.1 at 242 K) changes in the temperature range of 202−242 K, while the multiplet (δ = −46.8 at 242 K) is unchanged in all of the measured spectra (Figure 6).

The changes in the spectra suggest an intermolecular equilibrium process (Scheme 1) and intramolecular dynamics (Scheme 2). The changes in the ratio of intensities between minor and major resonances are in agreement with the equilibrium of **1** (minor resonances) and **1**·hmpa (major resonances) (Scheme 1). For the intramolecular dynamics, three mechanisms participating in the decoalescence of the two **1**·hmpa resonances during cooling have been considered: (1) The dynamics of the barium ion on the fluorine surface of the $[(C_5Me_5)_2Ti_2F_7]^-$ ligand (Scheme 2a). (2) The half-rotation of the $[(C_5Me_5)_2Ti_2F_7]^-$ ligand around its 2-fold axis (Scheme 2b). All of the seven fluorine atoms of the $[(C_5Me_5)_2Ti_2F_7]^-$ ligand in **1**·hmpa are chemically nonequivalent. The averaging to the single F_a, F_b, and F_c resonances could be achieved by the proposed half-rotation. Structurally similar compounds $[Ca\{(C_5Me_4Et)_2Ti_2F_7\}_2(L)]$ (L = THF, dioxane, hmpa) exhibit only single F_a, F_b, and F_c resonances down to 252 K.[12,18] Two F_a, F_b, and F_c resonances would be expected also for calcium compounds, if the chemical nonequivalence was responsible for the splitting of the F_a and F_b resonances in **1**·hmpa. Therefore, this half-rotation mechanism of dynamics is unlikely. (3) The

(16) Hartke, B. *Angew. Chem., Int. Ed.* **2002**, *41*, 1468−1487.

(17) The molar ratio was obtained from the integral ratio for hmpa and C_5Me_5 protons in the ^{1}H NMR spectrum.

(18) Demšar, A.; Perdih, F.; Petrič, A.; Pevec, A.; Petriček, S. *Acta Chim. Slov.* **1999**, *46*, 185−191. (b) Pevec, A.; Demšar, A.; Gramlich, V.; Petriček, S.; Roesky, H. W. *J. Chem. Soc., Dalton Trans.* **1997**, 2215 and 2216.

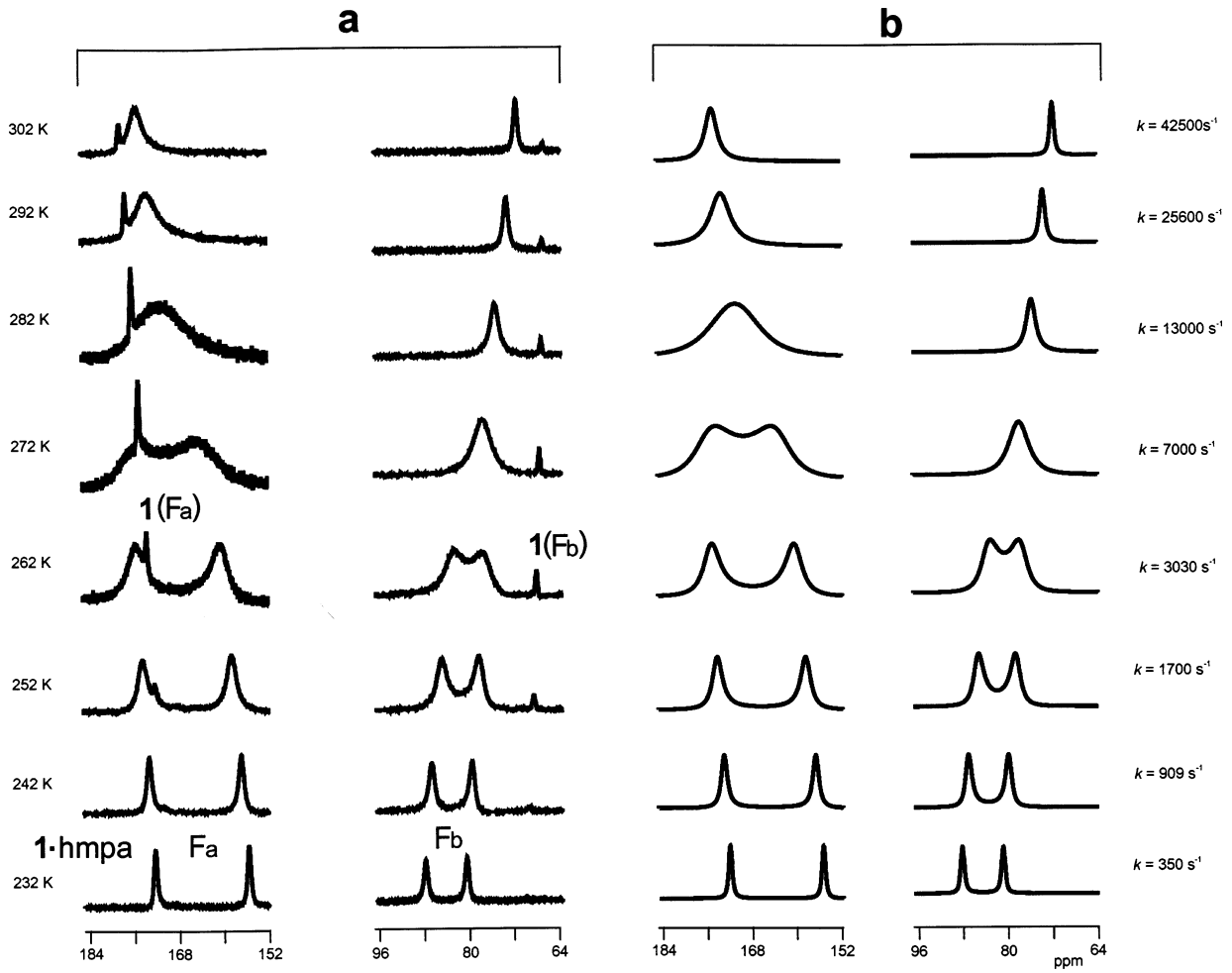

Figure 5. Observed (a) and simulated (b) ^{19}F NMR spectra of the hmpa/**1**·hmpa (6:1 molar ratio) toluene-d_8 solution (0.02 M **1**·hmpa) in the range of the F_a and F_b resonances.

moving of coordinated hmpa between two positions found as disorder over the 2-fold rotation axis in the solid-state structure. This dynamics is also unlikely. As proposed for mechanism 2, the different distances of fluorine atoms to the coordinated hmpa do not induce the splitting of the fluorine resonances.

Four ^{19}F NMR resonances observed for **1**·hmpa resemble the resonances of $[(C_5Me_5)_2Ti_2F_7]^-$ coordinated to lithium,[19] calcium,[12] and lanthanum.[9] The resonances are ascribed to the following fluorine atoms (in the order of decreasing frequencies; see Scheme 1): terminal (F_a), Ti−F−Ba doubly bridging (F_b), triply bridging (F_c), and Ti−F−Ti doubly bridging (F_d). Four fluorine resonances are expected also for **1**. Two of them (F_a and F_b) were observed as minor resonances; the F_c and F_d resonances are partially observed close to the F_c and F_d resonances of **1**·hmpa in the 272 K spectrum (Figure 6) but are hidden at higher temperatures by the resonances of **1**·hmpa.

The ^{1}H NMR spectrum of hmpa/**1**·hmpa (6:1 molar ratio) at 302 K shows doublet resonances of free and (as a shoulder, shifted by 0.007 ppm) coordinated hmpa in slow exchange.

Complexation Equilibrium. The equilibrium of **1** and **1**·hmpa is similar to that observed with $[Ca\{(C_5Me_4Et)_2Ti_2F_7\}_2]$ and $[Ca\{(C_5Me_4Et)_2Ti_2F_7\}_2(hmpa)]$.[18] The equilibrium constants were calculated from the ratio of intensities of the F_b resonances of **1**·hmpa and **1** in the temperature range of 242−302 K. The equilibrium constants [$K = C_{\mathbf{1}\cdot hmpa}/(C_{\mathbf{1}}C_{hmpa})$, in units of L mol^{-1}] 367 (242 K), 267 (252 K), 254 (262 K), 203 (272 K), 128 (282 K), 104 (292 K), and 97 (302 K) resulted in $\Delta H = -14.2(5)$ kJ mol^{-1}, $\Delta S = -9.3(5)$ J mol^{-1} K^{-1}, and $\Delta G_{298} = -11.4(5)$ kJ mol^{-1}.

Barium-Ion Dynamics. The intramolecular dynamics (Scheme 2a) proposes the barium ion, equidistant to two F_c resonances but closer to one of both of the F_b resonances, to move between these two atoms. Seven fluorine resonances are expected in the slow-exchange limit from the nonsymmetric $Ba\{(C_5Me_5)_2Ti_2F_7\}$ moiety with a small chemical-shift difference between both of the F_c resonances and a larger difference between both of the F_a and both of the F_b resonances. The ^{19}F NMR spectra were simulated according to this model, which results in the averaging of two F_a, two F_b, and two F_c resonances to single F_a, F_b, and F_c resonances.

The exchange rate constants were determined by the simulation of the F_a and F_b resonances (Figure 5b).[20] The line shapes of F_c (above 243 K) and F_d resonances of

(19) Demšar, A.; Pevec, A.; Golič, L.; Petriček, S.; Petrič, A.; Roesky, H. W. *Chem. Commun.* **1998**, 1029 and 1030. (b) Pevec, A.; Perdih, F.; Košmrlj, J.; Modec, B.; Roesky, H. W.; Demšar, A. *Dalton Trans.* **2003**, 420−425.

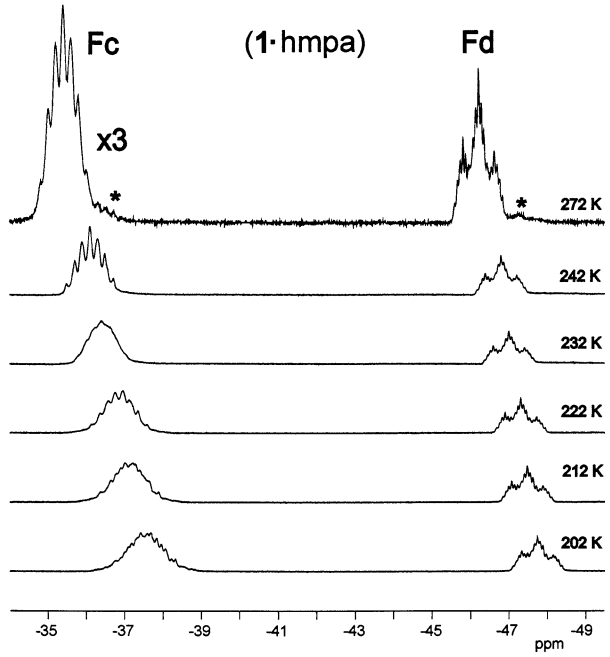

Figure 6. Selected VT ^{19}F NMR spectra of the hmpa/**1**·hmpa (6:1 molar ratio) toluene-d_8 solution in the range of the F_c and F_d resonances (see Scheme 1). Asterisks indicate the F_c and F_d resonances of **1**.

Scheme 1

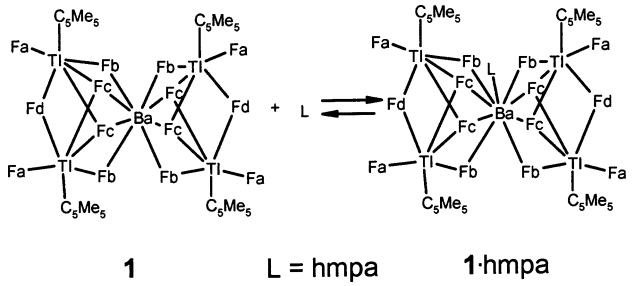

Scheme 2

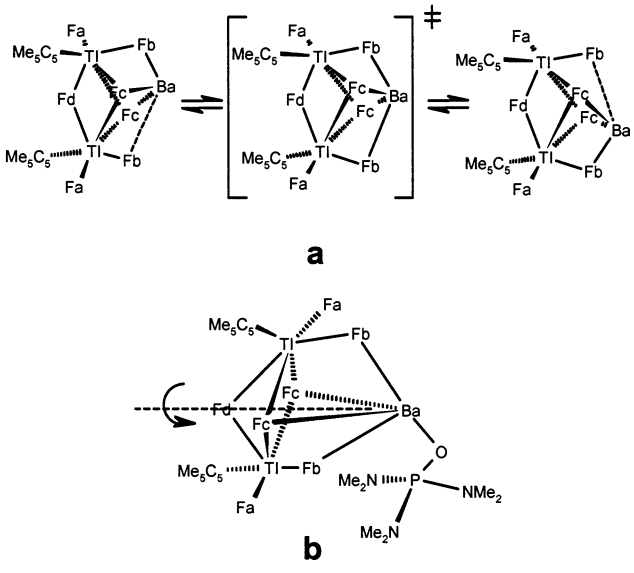

1·hmpa are very similar to the corresponding resonances of [Ca{$(C_5Me_4Et)_2Ti_2F_7$}$_2$].[12] The F_a and F_b resonances of **1**·hmpa for the slow-exchange limit were therefore approximately simulated (quintet with $J = 44$ Hz for F_a, triplet with $J = 75$ Hz for F_b) to the shape of the corresponding resonances in [Ca{$(C_5Me_4Et)_2Ti_2F_7$}$_2$]. Activation parameters are calculated from the Eyring plot (Figure 7) to be $\Delta H^{\ddagger} = 37.6(5)$ kJ mol^{-1} and $\Delta S^{\ddagger} = -32.3(5)$ J mol^{-1} K^{-1}. The negative activation entropy is in agreement with the additional bonding of the barium ion in the proposed transition state. The activation enthalpy is similar to that for the sliding of the zinc ion on the oxo surface of doubly deprotonated *p-tert*-butylsulfonylcalix[4]arene [45(1) kJ mol^{-1}].[21] The changes of the F_c resonances in the VT NMR spectra are in agreement with the proposed dynamics and calculated activation parameters. These resonances can be approximately simulated in the temperature range of 202−242 K (with the exchange rates calculated from the Eyring plot) as the exchange of two septets separated by 0.32 ppm.

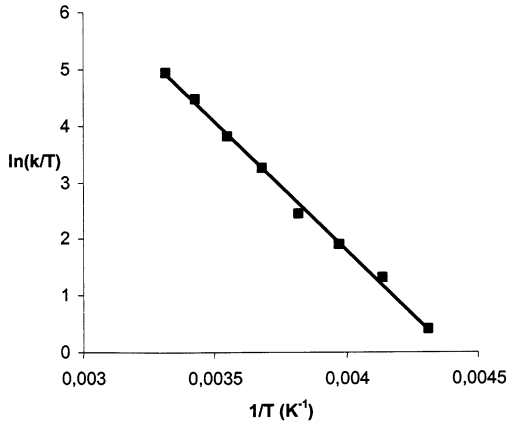

Figure 7. Eyring plot of the barium-ion dynamics (Scheme 2a) calculated from the VT ^{19}F NMR spectra of the hmpa/**1**·hmpa toluene-d_8 solution.

The F_a and F_b resonances of **1**·hmpa remain singlets during cooling to 212 and 222 K (not shown in Figure 5). However, the simulation of these spectra at 202 and 212 K using the model in Scheme 2a and exchange rate constants calculated from the Eyring plot gives multiplets. This may indicate an additional faster dynamics in **1**·hmpa. We speculate that hmpa and two [$(C_5Me_5)_2Ti_2F_7$]$^-$ ligands move (in a plate-tectonics manner) around the barium ion. The motion between the different mutual orientation of ligands with slightly different chemical shifts of fluorine resonances results in the disappearance of multiple structures of the fluorine atoms F_a and F_b on a ligand "boundary". The resonances of the F_c and F_d "inner" ligand atoms are less influenced by the dynamics and retain the multiplet structure. Two disordered positions of hmpa in the solid-state structure suggest that different orientations of the ligands in **1**·hmpa are possible.

Evaluation of the Equilibrium and the Dynamics. The comparison of the thermodynamic parameters for the coordination of the barium ion in **1** by hmpa [$\Delta H = -14.2(5)$ kJ mol^{-1}, $\Delta S = -9.3(5)$ J mol^{-1} K^{-1}, and $\Delta G_{298} = -11.4(5)$ kJ mol^{-1}] with those for the coordination of the calcium ion in [Ca{$(C_5Me_4Et)_2Ti_2F_7$}$_2$] by hmpa [$\Delta H =$

(20) Budzelaar, P. H. M. *gNMR*, version V 4.0.1; Ivorysoft: Oxford, U.K., 1997.

(21) Kajiwara, T.; Yokozawa, S.; Ito, T.; Iki, N.; Morohashi, N.; Miyano, S. *Angew. Chem., Int. Ed.* **2002**, *41*, 2076−2078.

$-25(1)$ kJ mol^{-1}, $\Delta S = -56.3(6)$ J mol^{-1} K^{-1}, and $\Delta G_{298} = -8.2(5)$ kJ mol^{-1}][18] shows a higher exothermicity of the calcium-ion complexation. The less negative entropy change for the barium-ion complexation can be explained by the intramolecular dynamics of **1**·hmpa that increases its entropy. The difference in the entropy change results in a significant difference in the free energy change and consequently in the higher formation constant for the barium compound ($K_{298} = 100$ L mol^{-1}) than that for the calcium compound ($K_{298} = 27$ L mol^{-1}). In other words, the nonrigid complex of the larger metal (Ba) with the weaker metal−ligand interactions is more stable than the analogous rigid complex of the smaller metal (Ca) with the stronger metal−ligand interactions. Such a difference in stability of the complexes could play a role in the recognition of cations of different sizes, for example, sodium and potassium in biological systems.

The ^{19}F NMR spectra of **1**·hmpa·(THF) at 302 and 222 K show four resonances with chemical shifts similar to the F_a, F_b, F_c, and F_d resonances of **1**·hmpa observed in the hmpa/**1**·hmpa solution. The 25 additional minor resonances at 222 K suggest the formation and equilibria of larger aggregates with lower symmetry in the absence of an excess hmpa. The aggregates could be similar to the intermediates in the formation of **2**.

Conclusions

Compounds **1**·hmpa·(THF) and **2**$[I_3]_2$·10(THF) show that the Ti-bonded F atoms are resistant to the formation of solid BaF_2 and are able to coordinate to the Ba^{2+} ion. Although the perovskite properties are due to the orientation of domains in the bulk, the preparation of discrete "perovskite" molecules or ions is an interesting target. The synthesis of **2**$[I_3]_2$·10(THF) suggests that such perovskite fragments could be self-assembled by incorporating a small B-type ion (added to the solution) in the empty site in the center of **2**. VT ^{19}F NMR spectroscopy gives insight into the coordination and dynamics of the barium ion in **1**·hmpa in solution.

Acknowledgment. This work was supported by Grant PS-0511-0103 from the Ministry of Education, Science and Sport, Republic of Slovenia. Thanks are given to Bogdan Kralj for mass spectrum measurements and Prof. Alojz Demšar for helpful discussions.

Supporting Information Available: X-ray crystallographic files in CIF format for the structure determination of **1**·hmpa·(THF) and **2**$[I_3]_2$·10(THF). This material is available free of charge via the Internet at http://pubs.acs.org.

IC035256V